Available online at www.sciencedirect.com
ScienceDirect
Trans. Nonferrous Met. Soc. China 24(2014) 1717−1729
Transactions of Nonferrous Metals Society of China
www.tnmsc.cn

Comparison of microstructural stability of IN939 superalloy with two different manufacturing routes during long-time aging

M. R. JAHANGIRI[1], H. ARABI [2], S. M. A. BOUTORABI [2]

1. Metallurgy Department, Niroo Research Institute, Tehran 14686, Iran;
2. School of Metallurgy and Materials Engineering, Iran University of Science and Technology, Tehran 16846-13114, Iran

Received 24 September 2013; accepted 22 January 2014

Abstract: Microstructural stability of IN939 superalloy with two different manufacturing routes was investigated during long-term aging at elevated temperatures by light optical microscope (OM) and scanning electron microscope (SEM) equipped with an EDS system. The results show that the coarsening behavior of γ' particles is primarily impacted by the initial heat treatment conditions, and the effect of the prior manufacturing route (casting or hot forming) is found to be insignificant, if any, on the γ' particles coarsening kinetics. In the temperature range of 790−827 °C, IN939 cast/wrought-HT2 alloys have more microstructural stability, while in the temperature range of 827−910 °C, the initial heat treatment marked as HT1 provides more stable microstructure for the cast or wrought IN939 superalloy.

Key words: nickel-based superalloy; IN939 superalloy; long-term coarsening; manufacturing route; heat treatment; γ' particles; carbides

1 Introduction

Superalloys are frequently utilized in the industry as high temperature materials in the form of cast or wrought components. Some superalloys are used as cast components with the same chemical composition as well as wrought forms.

One of the major characteristics of superalloys is their microstructural stability during exposure to high temperatures for a long time. Although, so much research has been performed on the effects of short-term or long-term aging on the microstructural changes of superalloys [1−6], but in all of these studies, either a cast or a wrought superalloy has been studied solely. As far as the authors know, no published data have evaluated and compared the microstructural changes of a superalloy with two different manufacturing routes (cast or wrought) during long term aging at high temperatures.

The finer grains of wrought alloys denote that they have more grain boundaries in a unit volume of the material. Grain boundaries as well as subgrain boundaries act as preferred sites for diffusion of alloying elements in the microstructure, and consequently, they can influence the coarsening rate of γ' particles [6−8]. Furthermore, the density of twin boundaries and stacking faults is much more in the microstructure of wrought alloys. Hence, increasing of these lattice defects can lead to more diffusivity of alloying elements, and this may in turn increase the γ' particles growth rate in the wrought alloys.

Initial heat treatments have significant effects on the γ' particles size and distribution, and hence can influence the coarsening behavior of γ' precipitates to a great extent. Scattered published data [2,5,6,9−12] showed that various initial γ' particles size and distribution resulting from various heat treatments may lead to different coarsening behavior during long-time aging at different temperatures. Moreover, there is no any published report on the microstructural stability of IN939 superalloy with different initial heat treatments.

Accordingly, the aim of this research was to study the effect of primary manufacturing method (cast or wrought alloy with different heat treatments) of a unique superalloy on the microstructural stability during long-time aging at high temperatures. Particularly, the effect of prolonged aging at elevated temperatures was investigated on the activation energy and coarsening rate coefficient of γ' particles, as well as the MC carbides stability for a fixed superalloy with two different

Corresponding author: M. R. JAHANGIRI; Tel: +98-21-88079401-6; Fax: +98-21-88078296; E-mail: mjahangiri@nri.ac.ir
DOI: 10.1016/S1003-6326(14)63245-3

manufacturing routes.

In this work, IN939 superalloy was studied. IN939 is a precipitation-hardened nickel-based superalloy, which is now mainly used for manufacturing of high temperature cast components such as gas turbine blades/vanes, fuel nozzles and turbine casings [13,14]. It has excellent mechanical properties and corrosion resistance simultaneously. Recently, JAHANGIRI et al [15,16] have developed wrought version of this alloy for applications such as gas turbine disks, seals, rings and casings, and fasteners.

2 Experimental

The materials used in this study were obtained via casting or hot rolling, and the complete manufacturing processes of these materials have been given in the previous publications [15,17]. After casting or rolling, various cast or wrought specimens with the same chemical composition (Table 1) were cut from the initial materials, and were heat treated in accordance with Table 2.

Table 1 Chemical composition of IN939 superalloy used in the present work (mass fraction, %)

C	Co	Cr	Ti	Al	W	Ta
0.144	19.25	22.38	3.65	1.99	1.97	1.45
Nb	Zr	B	P	S	Ni	
0.99	0.09	0.011	0.002	0.001	Bal.	

Table 2 Initial conditions of IN939 superalloy used in this work and related samples codes

Manufacturing method	Heat treatment	Sample code
Casting	(1150 °C, 4 h)+(1000 °C, 6 h)+(900 °C, 24 h)+(700 °C, 16 h)	Cast-HT1
	(1150 °C, 4 h)+(850 °C, 24 h)	Cast-HT2
Hot rolling	(1150 °C, 4 h)+(1000 °C, 6 h)+(900 °C, 24 h)+(700 °C, 16 h)	Wrought-HT1
	(1150 °C, 4 h)+(850 °C, 24 h)	Wrought-HT2

These heat treated specimens were exposed to three temperatures of 790, 850 and 910 °C for different periods (from 250 to 1500 h). These aging temperatures were selected as relatively low, medium and high temperatures to bound service temperatures of the alloy in power generation gas turbine applications. After aging, the microstructures of specimens were studied by light optical microscope (OM) and scanning electron microscope (SEM). The SEM was equipped with an energy dispersive X-ray spectrometer (EDS) system.

In this study, the Clemex software was used to measure the average size of γ' particles, as well as the volume fraction of these precipitates. The reported γ' particle sizes are the average values from the measurements made on six SEM micrographs of each sample. These micrographs were taken from the dendrite cores as well as the interdendritic regions of the cast-HT alloys microstructures.

3 Results and discussion

3.1 Overall microstructural changes and MC carbides transformation

The chemical composition of the IN939 superalloy used in this work is given in Table 1. Various micrographs in Fig. 1 show typical microstructures of IN939 alloy in the as-cast condition (Fig. 1(a)) and after HT1 heat treatment (Figs. 1(b)−(d)). In the cast condition, the alloy has a dendritic microstructure. The microstructure of the cast specimens includes the matrix γ together with the other phases such as γ' particles, MC carbides, and some η phases [17,18]. It is found that the elements Ti, Nb, Ta, and Zr are segregated to the interdendritic regions, while Cr is segregated to the dendrite cores [17]. Al element does not show significant segregation.

After HT1 heat treatment (Fig. 1(b)), the degree of segregation in the microstructure decreases to some extent in comparison with the as-cast microstructure, but there still exists relatively large heterogeneity between the dendrite cores and the interdendritic regions. This leads to various γ' particles size in different regions of the microstructure, and as mentioned in Section 2, the average size and distribution of γ' particles were measured on micrographs taken from the different regions of the microstructure and these average values were used in the analysis of the results.

Various MC carbides are observed within the grains or on the grain boundaries of the cast or cast-HT1 specimens (Figs. 1(a)−(e)). These MC-type carbides are enriched in Ti, Ta, and Nb elements. Some Cr-rich $M_{23}C_6$ carbides are also observed at the grain boundaries.

Figure 2 shows the microstructures of the cast IN939 superalloy after different initial heat treatments. Figures 2(a) and (b), which are related to cast-HT1 specimens, show that the alloy has coarse grains with approximate dimensions of (2±1) mm. The dendritic form of the microstructure is clear, and there is a considerable amount of inhomogenity and segregation of alloying elements in the microstructure. Quantitative metallography showed that the volume fraction of γ' precipitates is about 35% in these specimens, and the average size of these particles is around 121 nm.

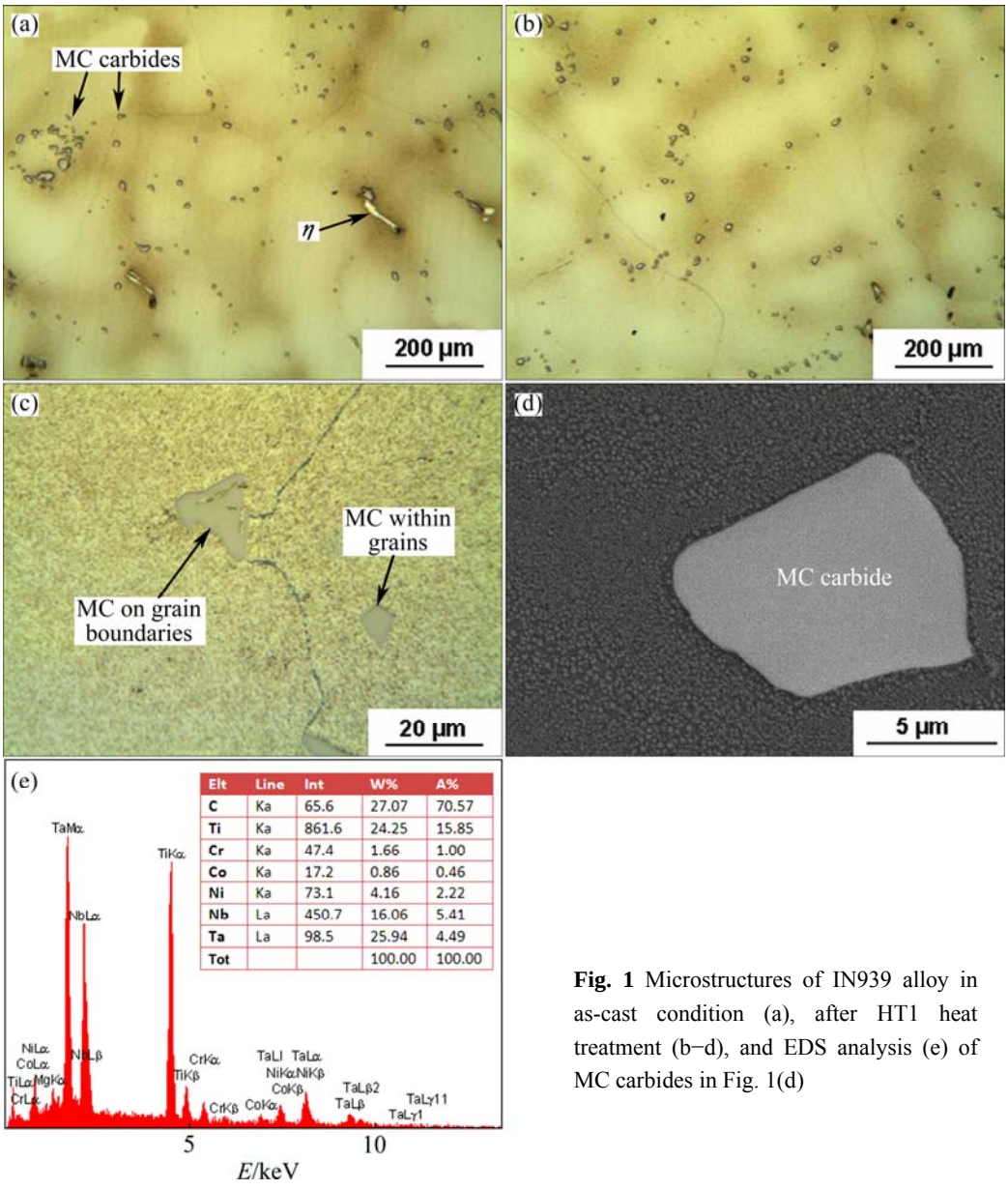

Fig. 1 Microstructures of IN939 alloy in as-cast condition (a), after HT1 heat treatment (b−d), and EDS analysis (e) of MC carbides in Fig. 1(d)

The microstructures of the specimens marked as cast-HT2 (Figs. 2(c) and (d)) indicate that these specimens have coarse grains and microscopic segregations as cast-HT1 specimens. The major difference between the cast-HT1 and cast-HT2 specimens is the size of γ' precipitates in the microstructures. The average γ' particle size is 66 nm for cast-HT2 specimen.

The main feature in the wrought and heat treated specimens is their microstructures with fine grains in the range of 100 μm containing numerous annealing twins (Figs. 3(a) and (c)). The results show that the grain size of the wrought and heat treated specimens is much finer than that of the cast and heat treated specimens. This indicates that the recrystallization has occurred during hot working or heat treating cycles. Because IN939 superalloy has high amounts of Co and Cr in its chemical composition, it has low stacking fault energy (SFE) [19]. At high temperatures, alloys with low SFE can easily undergo dynamic recrystallization during hot deformation processes, and this can lead to fine microstructures [20,21].

Depending on the applied heat treatment, wrought samples have two kinds of γ' precipitates with two sizes and morphologies. Larger precipitates existing in wrought-HT1 samples are mainly cubic (Fig. 3(b)), while the smaller ones in the wrought-HT2 specimens are rather spherical (Fig. 3(d)). Larger precipitates have formed during high-temperature aging at 900−1000 °C, while the finer ones have precipitated during lower-temperature aging at 850 °C. The average size of the γ' precipitates in the microstructure of wrought-HT1 and

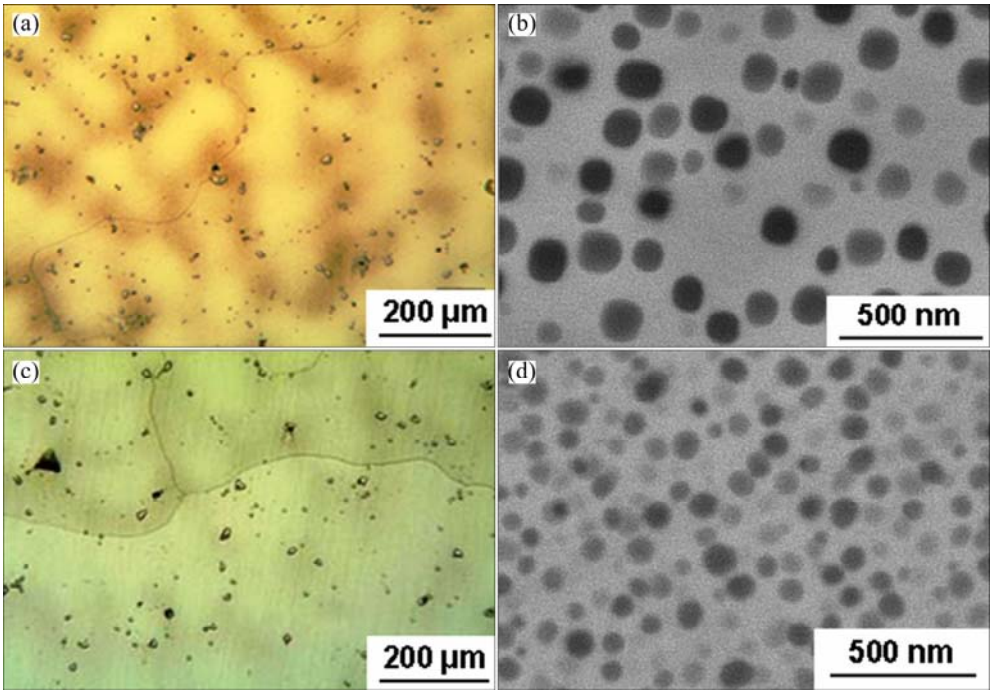

Fig. 2 Microstructures of cast IN939 superalloy samples after initial heat treatments: (a, b) Cast-HT1; (c, d) Cast-HT2

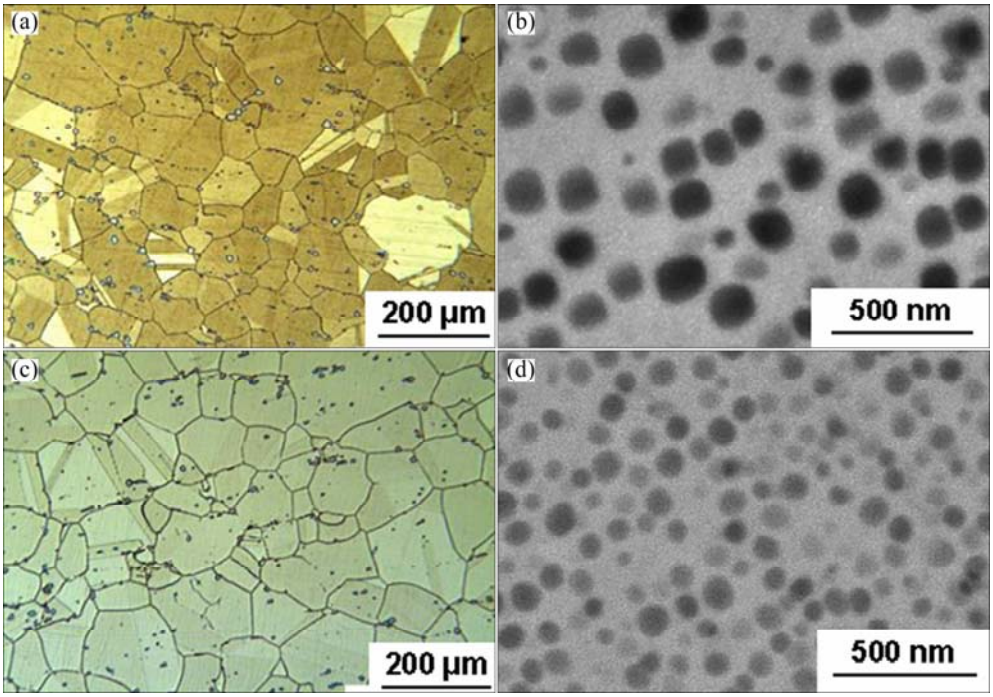

Fig. 3 Microstructures of wrought IN939 superalloy samples after initial heat treatments: (a, b) Wrought-HT1; (c, d) Wrought-HT2

wrought-HT2 samples are 132 nm and 73 nm, respectively.

Figure 4 shows the microstructures of cast-HT2 samples after exposure at 790 °C for 1500 h. The significant point about the microstructural changes of γ' precipitates for cast-HT2 samples at this temperature is that the initial spherical shape of these particles remains almost unchanged up to a long time. Only for samples aged at this temperature for 1500 h, both spherical and cubic morphologies are observed together (Fig. 4(c)).

For these samples, a platelet or blocky phase was detected with a chemical composition like the η phase in adjacent to MC carbides at some of the grain boundaries (Figs. 4(d) and (e)). At first, it was not specified whether this phase had been present in the initial microstructure, or it was formed during aging at 790 °C. Other results in

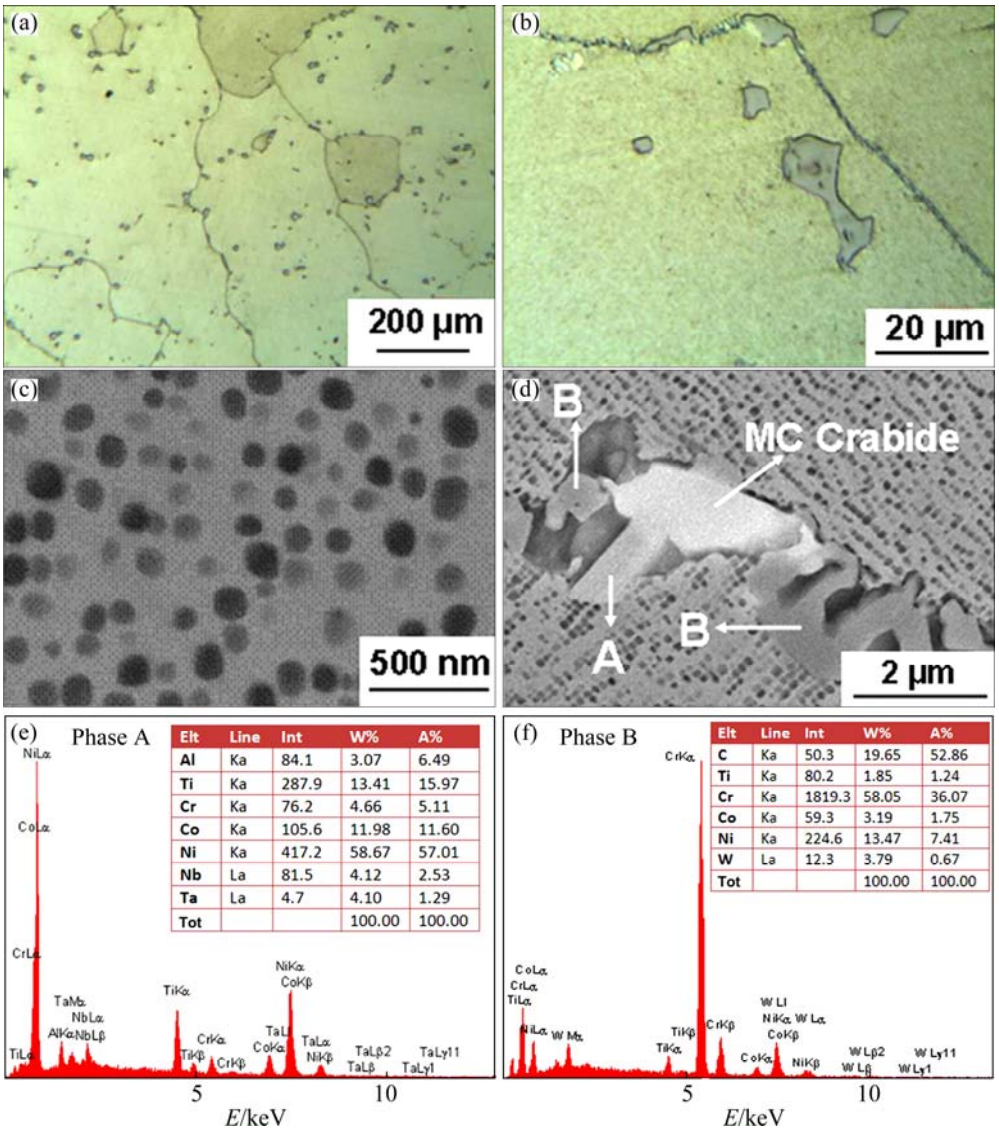

Fig. 4 Microstructures of cast-HT2 specimens after aging at 790 °C for 1500 h: (a, b) Optical microstructures; (c, d) SEM microstructures showing γ' precipitates distribution and MC carbides transformation; (e, f) EDS analysis of phases A and B in Fig. 4(d)

this work showed that this η phase was formed during the decomposition of MC carbides at 790 °C. In addition to η phase, Cr-rich carbides were also observed around the decomposed MC carbides, as well as along the grain boundaries (Figs. 4(d) and (f)).

Figures 5(a)−(c) show the microstructural changes of wrought-HT1 samples after aging for 1500 h at 790 °C. As shown, the changes in the size and morphology of γ' particles are small. After holding for 1500 h at this temperature, MC carbides within the grains show no significant change, while MC carbides at the grain boundaries undergo some degrees of microstructural transformation (Figs. 5(b) and (d)). It seems that the differences in the kinetics of MC carbides decomposition within the grains or at the grain boundaries have been arisen from the more diffusivity of the alloying elements at the grain boundaries.

As shown in Fig. 5(d), MC carbides at the grain boundaries have been transformed at the interface of MC/matrix to Cr-rich carbides such as $Cr_{23}C_6$ and a new phase (compared with Figs. 1(c) and (d)). The chemical composition of the new phase (phase B in Fig. 5(d)) is similar to that of the η phase with general formula Ni_3Ti (Fig. 5(f)). It should be pointed out that the η phase in IN939 superalloy contains some additional elements such as Ta, Nb and Al [18].

According to the published reports [22,23], the η phase can be formed at low temperature in high-Ti containing superalloys by the transformation of MC carbides. The possible equation can be expressed as follows:

$$MC+\gamma \rightarrow M_{23}C_6+\eta \quad (1)$$

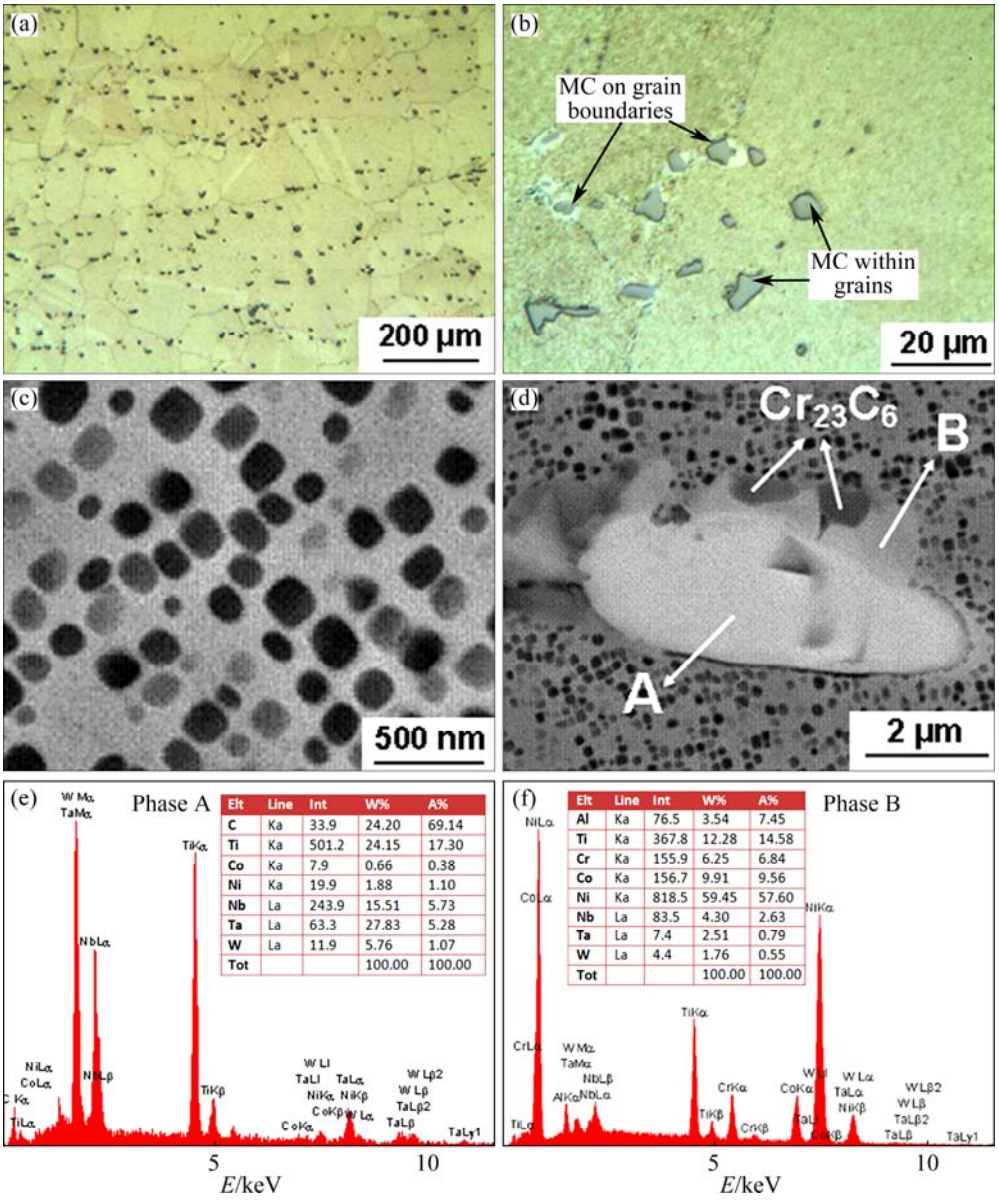

Fig. 5 Microstructures of wrought-HT1 specimens after aging at 790 °C for 1500 h: (a, b) Optical microstructures; (c, d) SEM microstructures showing γ' precipitates distribution and MC carbides transformation; (e, f) EDS analysis of phases A and B in Fig. 5(d)

Figure 6 shows the microstructural changes of cast-HT1 superalloy after aging at 910 °C for 1500 h. As shown in Fig. 6(a), there is still relatively large segregation between the dendrite cores and the interdendritic regions. A notable point is that, despite the existence of relatively large segregation between the dendrite cores and the interdendritic regions, no rafting is observed in the microstructures after aging for 1500 h (Fig. 6(b)).

Figure 6(c) shows the MC carbides transformation of these specimens after aging for 1500 h at 910 °C. This figure shows that the MC carbides in their interface regions with the matrix transform to Cr-rich carbides (Figs. 6(d) and (e)) and γ' phases. Under this temperature condition, no η phase is found around the MC carbides in the transformed regions. MC carbides transformation to Cr-rich carbides and γ' phases has been reported for many of the superalloys [5,24,25] and is formulated as follows:

$$MC+\gamma \rightarrow M_{23}C_6+\gamma' \quad (2)$$

Figures 7(a) and (b) show the microstructural changes of wrought-HT1 samples after aging for 1500 h at 910 °C. As shown in these figures, size and morphology of γ' particles have changed more than those observed at 790 °C (compared with Fig. 5). This is due to the higher diffusivity of γ'–former elements at 910 °C with respect to 790 °C [26]. It is also observed that for

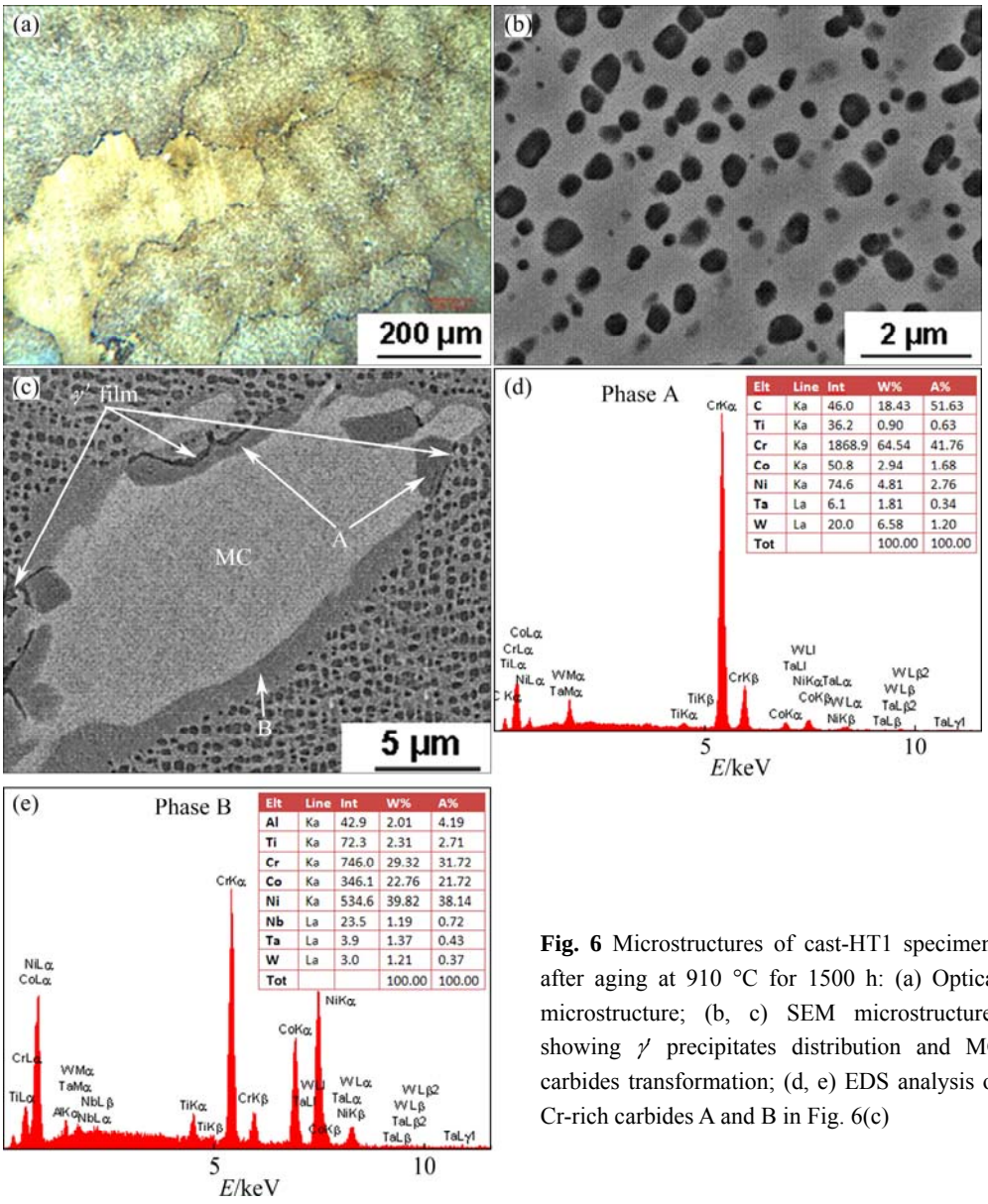

Fig. 6 Microstructures of cast-HT1 specimens after aging at 910 °C for 1500 h: (a) Optical microstructure; (b, c) SEM microstructures showing γ' precipitates distribution and MC carbides transformation; (d, e) EDS analysis of Cr-rich carbides A and B in Fig. 6(c)

the γ' particles located at the grain boundaries, the growth rates are much higher than those located within the grains. The reason is more diffusivity of alloying elements along the grain boundaries related to the grain interiors.

In this condition, MC carbides transform to Cr-rich carbides and γ' phases according to Eq. (2) (Figs. 7(c) and (e)). There is no evidence of η phase formation during MC carbides transformation at this temperature. The results at 850 °C also show that at this temperature, MC carbides transform to Cr-rich carbides and γ' phases. At 850 °C similar to 910 °C, no η phase is formed during the MC carbides transformation.

3.2 γ' particles coarsening rate and activation energy

Theory of Lifshitz, Slyosov and Wagner, which is briefly called LSW theory, states that if the growth of precipitates is controlled by diffusion, the average particle size increases according to the following equation [2−6]. This type of growth is also identified as Ostwald ripening.

$$\bar{a}^3-\bar{a}_0^3=Kt \text{ or } \bar{a}^3-\bar{a}_0^3=k^3t \quad (3)$$

In the above equation, $\bar{a}$, $\bar{a}_0$ and $K=k^3$ are the average particle size at time t, the average particle size at time $t=0$, and the rate constant or rate factor, respectively. Slope of the equation is equal to $K=k^3$, and it can be obtained from the following equation [2,3,6]:

$$K=(64\gamma DCV^2)/(9RT) \quad (4)$$

In the above equation, γ, D, C, V, R, and T are the interface free energy between the precipitates and matrix, the diffusion coefficient, the concentration of solute elements in equilibrium with a precipitate having an infinite radius, the molar volume of particles, the mole

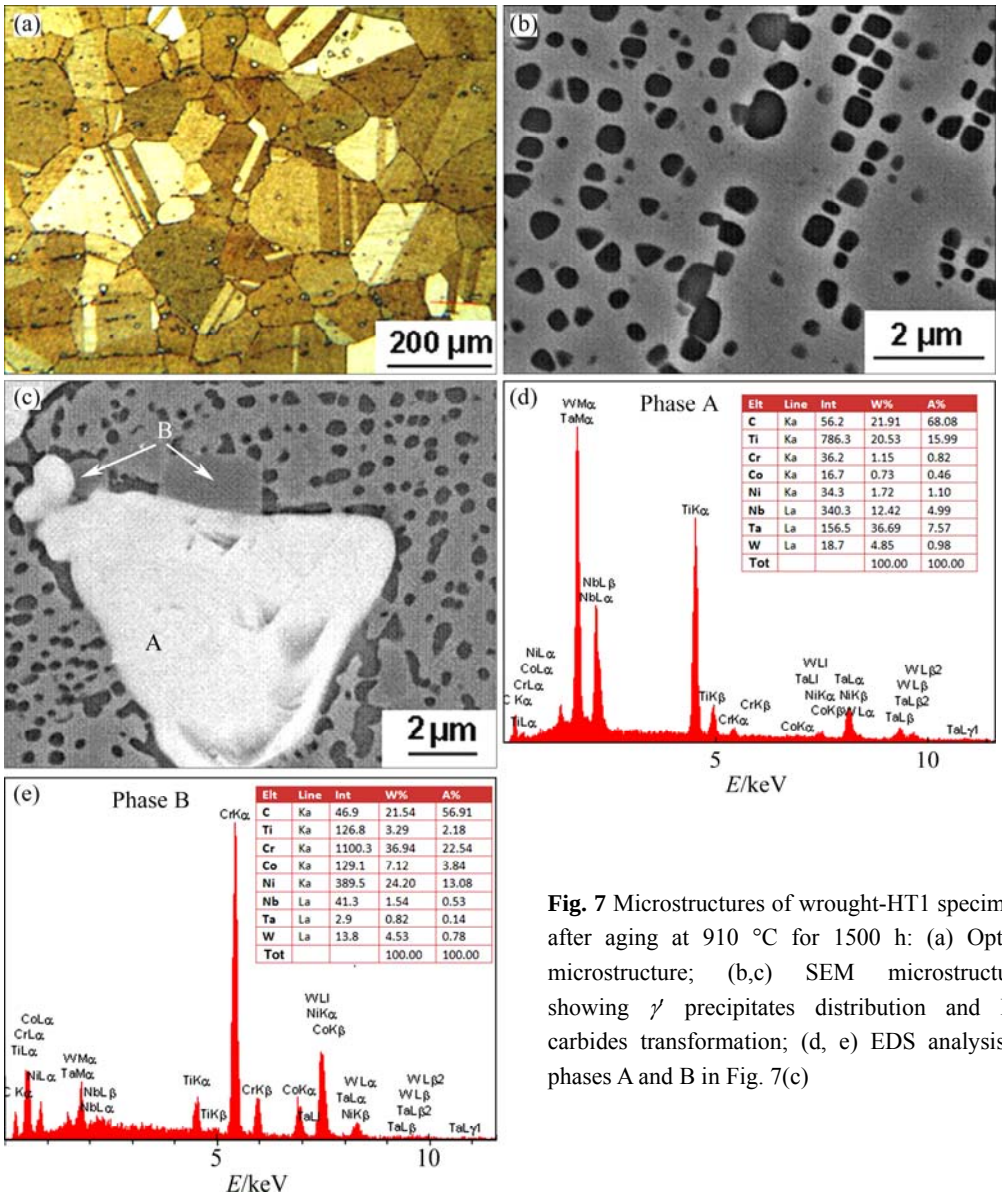

Fig. 7 Microstructures of wrought-HT1 specimens after aging at 910 °C for 1500 h: (a) Optical microstructure; (b,c) SEM microstructures showing γ' precipitates distribution and MC carbides transformation; (d, e) EDS analysis of phases A and B in Fig. 7(c)

gas constant, and the thermodynamic temperature. Equation (4) can be rewritten as follows:

$$\ln[k^3(T/C)]=\text{Constant}-[(Q/RT)] \quad (5)$$

Assuming that the parameter (T/C) has no significant influence [3,9], the activation energy for the growth of precipitates can be calculated by determining the slope of $\ln k^3$ versus $1/T$.

Figure 8 shows the results of changes in the size of γ' particles for cast or wrought samples with increasing aging time at 790, 850 and 910 °C, respectively. As can be seen, the plot of the cube of the average γ' precipitates size against the aging time is almost a straight line. This indicates that the growth of the γ' precipitates in cast or wrought IN939 superalloy with different heat treatments and different initial microstructures follows LSW equation at 790−910 °C and aging times up to 1500 h. This demonstrates that the diffusion of alloying elements in IN939 superalloy controls the coarsening behavior of γ' particles.

Using the plots of $\ln k^3$ versus $1/T$ (Figs. 9), the activation energy values for growth of γ' precipitates in the cast or wrought IN939 superalloy were calculated. These values as well as the γ' particles growth rate coefficients are given in Table 3.

The results show that in the cast or wrought IN939 superalloy, the activation energy of coarsening for the γ' particles is within the range of 266−290 kJ/mol. By comparing the activation energy for the growth of γ' precipitates in the IN939 superalloy with those values reported for Ni−Al alloys and other superalloys (240−280 kJ/mol) [2−6,9−12,27], it can be seen that the activation energy values obtained in this research are in the upper range of similar alloys. Diffusion controlled

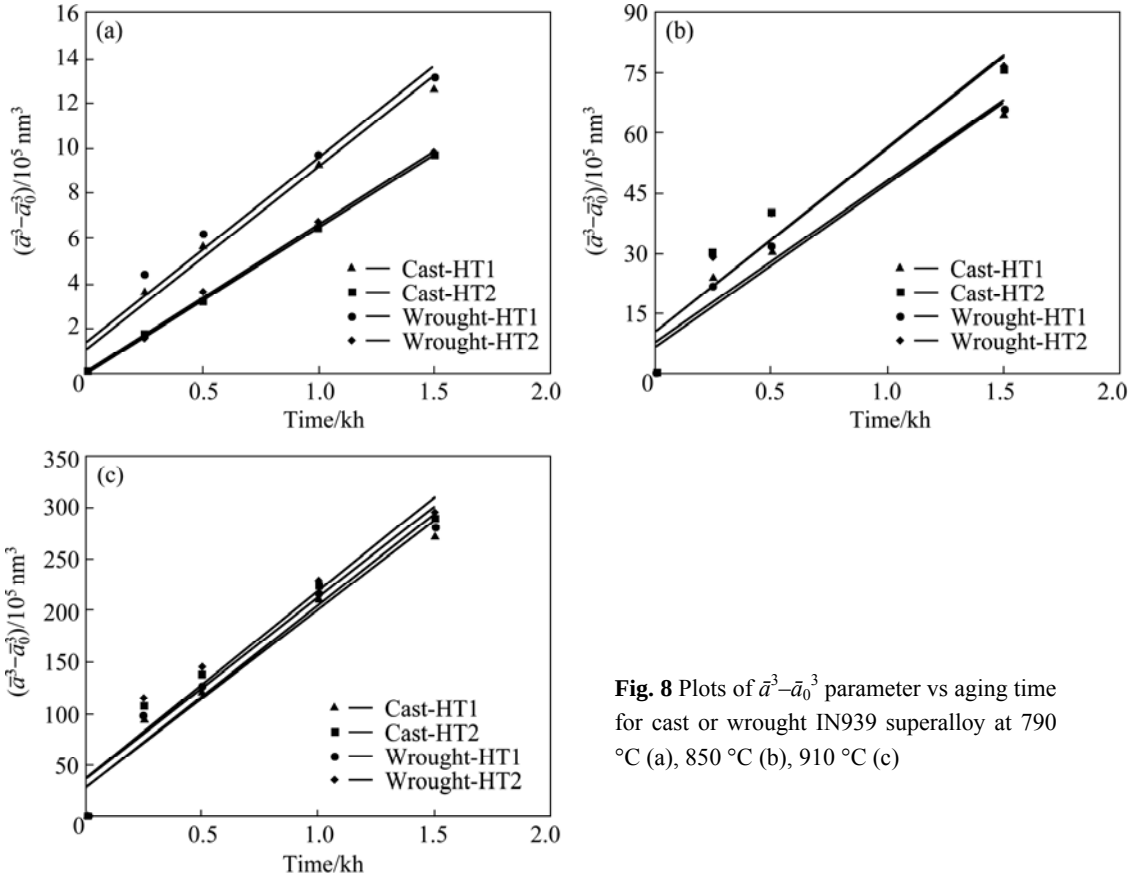

Fig. 8 Plots of $\bar{a}^3-\bar{a}_0{}^3$ parameter vs aging time for cast or wrought IN939 superalloy at 790 °C (a), 850 °C (b), 910 °C (c)

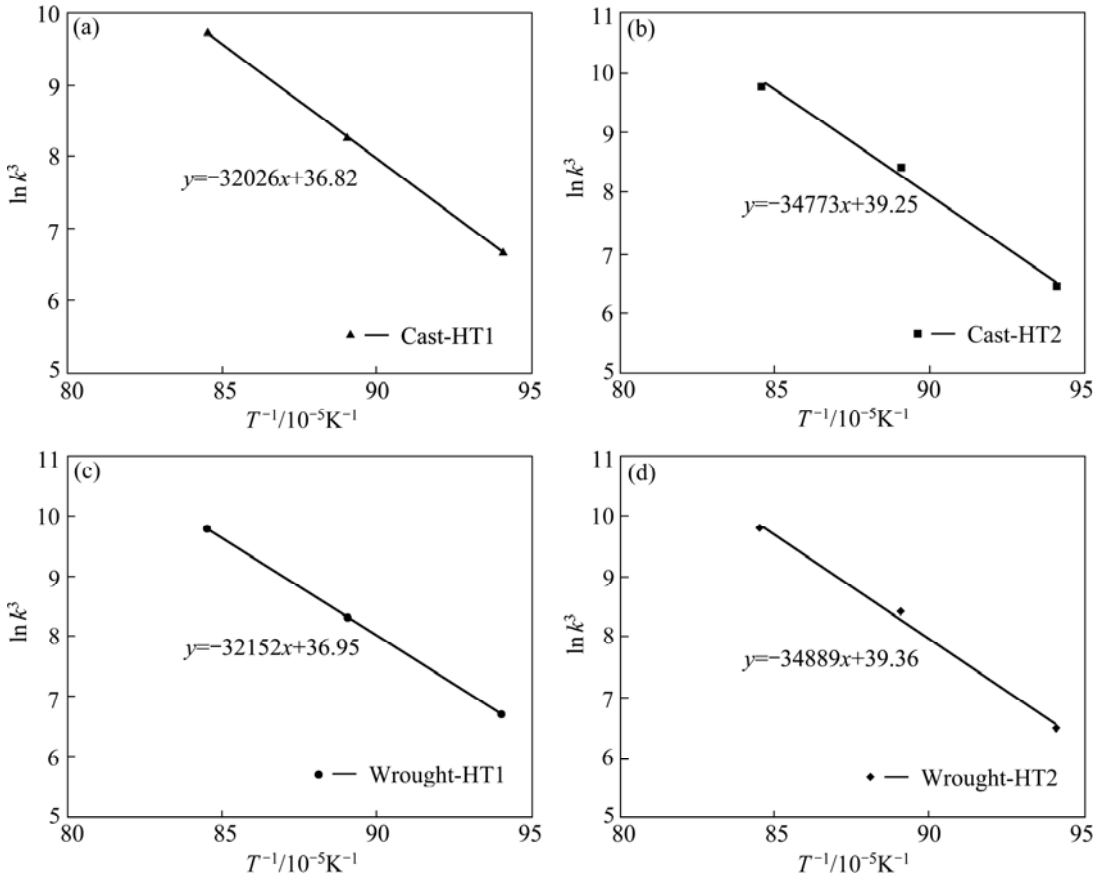

Fig. 9 Plots of ln k^3 vs 1/T for IN939 superalloy with different manufacturing routes

Table 3 Calculated γ' particle growth rate coefficients and activation energy values for IN939 superalloy with different manufacturing routes

Alloy code	Aging temperature/ °C	Aging time/ h	γ' growth rate coefficient/ ($nm^3 \cdot h^{-1}$)	γ' growth activation energy/ ($kJ \cdot mol^{-1}$)
Cast-HT1	790	0−1500	812.6	
Cast-HT1	850	0−1500	4017	266.28
Cast-HT1	910	0−1500	17271	
Cast-HT2	790	0−1500	647.2	
Cast-HT2	850	0−1500	4566	289.11
Cast-HT2	910	0−1500	17737	
Wrought-HT1	790	0−1500	820.1	
Wrought-HT1	850	0−1500	4069	267.32
Wrought-HT1	910	0−1500	17642	
Wrought-HT2	790	0−1500	653.4	
Wrought-HT2	850	0−1500	4604	290.1
Wrought-HT2	910	0−1500	18110	

models typically consider the diffusion of Al and Ti elements as the limiting factors for the growth of γ' particles in the superalloys. It has been shown that the presence of Ta, W, and Nb elements in superalloys can decrease the coarsening rate of γ' particles due to their low diffusivity in the γ matrix [3,28,29]. Because IN939 superalloy has relatively high amounts of slow diffusing elements, the activation energy for coarsening of γ' particles in this alloy is in the upper range of the published data. Moreover, it has been reported that the coarsening (ripening) rate of γ' particles in superalloys decreases as the Cr and Co contents of the alloy increased [23,30]. Consequently, these elements, which have high concentration in IN939 superalloy, reduce the solubility of Al and Ti in matrix, and hence decrease the γ' particles growth rate. The activation energy values obtained in this research are to some extent greater than those for diffusion of Ti in Ni (257 kJ/mol [6,27]) and diffusion of Al in Ni (269 kJ/mol [6,27]). Because the γ' phase composition in IN939 superalloy is mainly based on Ni, Co, Al, and Ti with the lower levels of Ta, Nb, and W [31], it can be concluded that the γ' particles coarsening in this alloy is mainly controlled by the reduced diffusion of Al and Ti atoms in the presence of the other alloying elements.

By comparing the coefficients of the coarsening rate of γ' precipitates in the cast or wrought IN939 superalloy at different temperatures, it can be found that the growth rate of the particles is very sensitive to the aging temperature of samples. An increase of 120 °C in aging temperature also increases the growth rate factor by 21−27 times. Based on Eqs. (4) and (5), one can say that such high increases in parameter K with temperature are related to the exponential dependency of the alloying elements diffusion on temperature.

On the basis of the results presented in Fig. 8 and Table 3, significant points can be drawn. An important point in this research is that the coefficients of the growth rate and activation energies for the coarsening of γ' precipitates for wrought and heat treated samples are almost similar to those obtained for cast and equivalent heat treated samples. In other words, the effect of the prior manufacturing route (casting or hot forming) is found to be insignificant on the overall coarsening behavior of the γ' particles.

Although the wrought samples have a finer grain microstructure with numerous twins, and a high density of stacking faults, but the coarsening rate coefficients of the γ' particles for wrought specimens are not significantly different from those of the cast specimens with the same heat treatment. This implies that the γ' particles coarsening in the cast or wrought IN939 superalloy is a continuous coarsening process which is controlled by volume diffusion of alloying elements. Therefore, grain boundaries, twins, and stacking faults have no significant effect on the particles coarsening behavior.

On the other hand, the initial heat treatment has a major influence on the coarsening kinetics of the γ' particles. At 790 °C, the coarsening rate factor for HT1 specimen is larger compared to that obtained for HT2 specimens. A reversed trend is observed at 850 °C, and at 910 °C, the coarsening rate constants are almost the same for all the specimens.

The variations of K vs temperature lead to distinct changes in the activation energy values, so that one may be able to explain some unexpected published results about the relationship between K and Q parameters [9−12]. In some of these references, the higher activation energy values have been associated with higher coarsening rate factors in a temperature range, while in the other references, the situation has been reversed.

To better clarify this subject, the results presented in Fig. 8 and Table 3 are replotted in Fig. 10. In this figure, the results are shown in two different temperature ranges of 790−850 °C (Figs. 10(a) and (b)) and 850−910 °C (Figs. 10(c) and (d)). By measuring the slopes of the lines, the activation energy values for growth of γ' particles are calculated and given in Table 4.

Figures 10(a) and (b) show that despite the constant values of the activation energy for specimens HT1 or HT2 in the temperature range of 790−850 °C, the coarsening rate coefficients have been changed. For example, although cast-HT2 alloy has lower coarsening rate coefficients in the temperature range 790−827 °C, it has higher coarsening rate constants in the temperature

Table 4 γ' particles growth rate coefficients and activation energy values for IN939 superalloys in two separate temperature ranges

Alloy code	Aging temperature/ °C	γ' growth rate coefficient/ ($nm^3 \cdot h^{-1}$)	γ' growth activation energy/ ($kJ \cdot mol^{-1}$)
Cast-HT1	790	812.6	264.35
Cast-HT1	850	4017	
Cast-HT2	790	647.2	323.19
Cast-HT2	850	4566	
Wrought-HT1	790	820.1	264.96
Wrought-HT1	850	4069	
Wrought-HT2	790	653.4	322.98
Wrought-HT2	850	4604	
Cast-HT1	850	4017	268.5
Cast-HT1	910	17271	
Cast-HT2	850	4566	249.82
Cast-HT2	910	17737	
Wrought-HT1	850	4069	270.05
Wrought-HT1	910	17642	
Wrought-HT2	850	4604	252.12
Wrought-HT2	910	18110	

range 827−850 °C compared to cast-HT1 alloy. It is reiterated that the cast-HT2 alloy has higher activation energy (which is related to slope of the Arrhenius plot) for the γ' particles coarsening in the entire temperature range 790−850 °C.

In the temperature range 850−910 °C, the activation energy of γ' particles growth for HT1 specimens is more than that of HT2 specimens (Figs. 10(c) and (d), and Table 4). Also, the coarsening rate coefficients are lower for samples HT1, although the K parameters of two heat treatments come closer together as the temperature increases.

Figure 11 shows a schematic summary of the results obtained in this study. This figure shows that in the temperature range of T_1−T_2, cast/wrought alloys HT2, which have higher activation energy values for γ' particles coarsening, also have lower coarsening rate coefficients. In the temperature range of T_2−T_3, where the alloys HT1 have lower activation energies, these alloys have also lower growth rate constants. In the temperature range of T_3−T_4, alloys HT1, which have higher activation energy values for γ' particles coarsening, also have lower coarsening rate coefficients. This implies that there is no expected relationship between the parameters K and

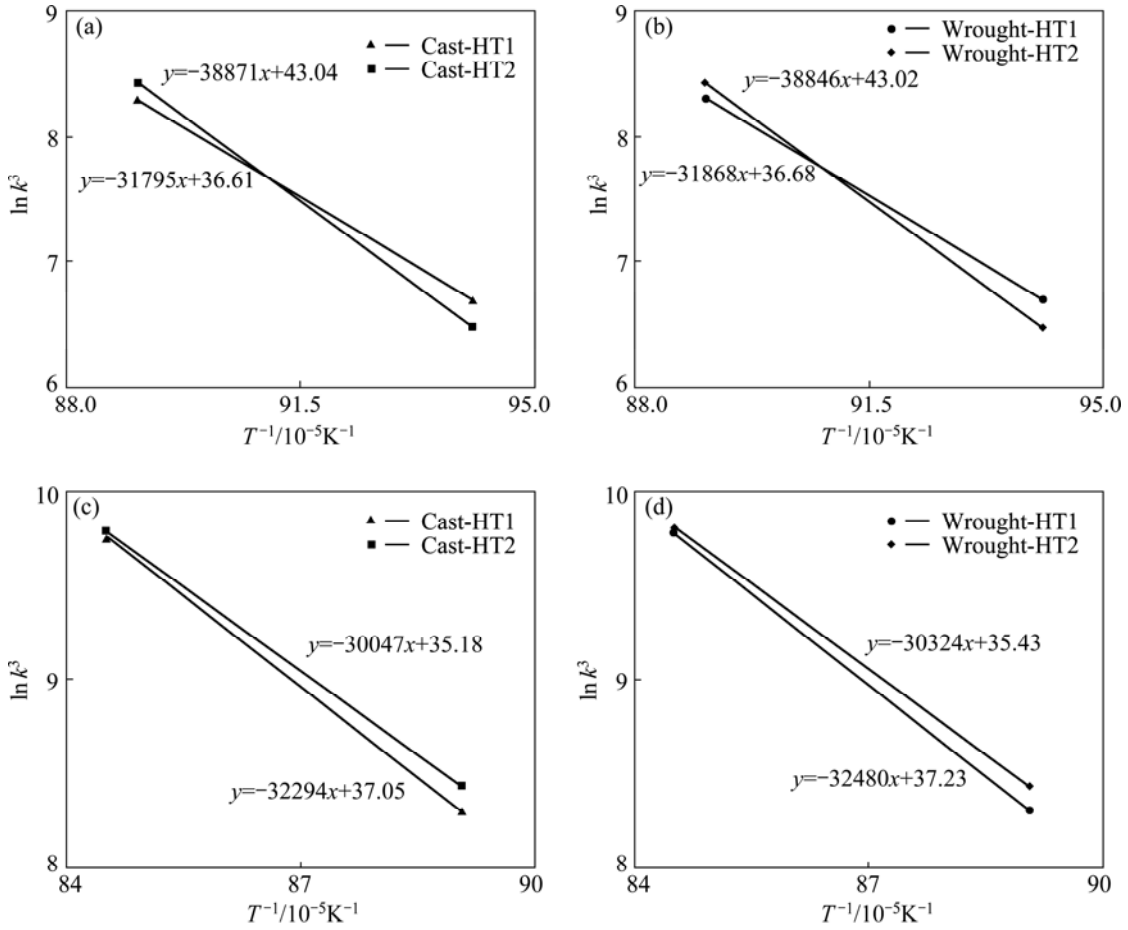

Fig. 10 Plots of ln k^3 vs $1/T$ for IN939 superalloy with different manufacturing routes in two separate temperature ranges: (a, b) 790−850 °C; (c, d) 850−910 °C

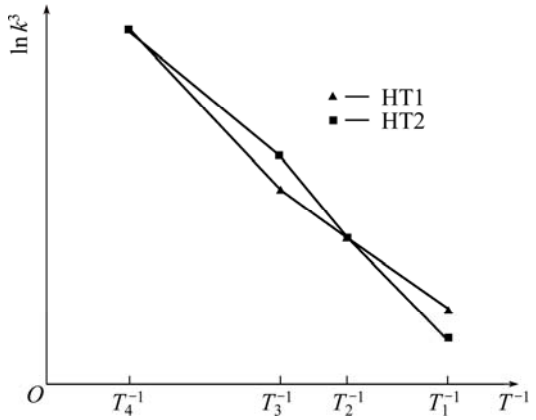

Fig. 11 Schematic summary of results obtained in present work about relationship between K and Q parameters, i.e., ln k^3 vs T^{-1}, for different HT alloys

Q in the temperature range of T_2−T_3.

On the basis of the above results, it can be concluded that in the temperature range of 790−827 °C, IN939 cast/wrought-HT2 alloys have more microstructural stability, while in the temperature range of 827−910 °C, the initial heat treatment marked as HT1 provides lower growth rate constants and more stable microstructures for cast or wrought IN939 superalloy.

To explain the above results, it is necessary to look again at the aging cycles during initial heat treatments of these alloys (Table 2). The last aging step for specimens HT1 was carried out at 700 °C. The result of this aging process is the formation of very fine particles in the space between the coarser γ' particles formed during the previous aging cycles [15,31]. These very fine particles have no sufficient stability during aging at high temperatures. They are dissolved at relatively low temperatures, and participate in the coarsening process of the larger γ' particles. In contrast, the aging cycle for specimens HT2 was performed at 850 °C. Hence, the γ' particles in these specimens are more stable at lower temperatures.

The above results show that during the long-term aging of the samples at relatively low temperatures (790−827 °C), the microstructural stability of the specimens HT2 is higher than that of the specimens HT1. On the other hand, because of the use of higher temperatures during the early stages of aging heat treatments for specimens HT1 (1000 °C and 900 °C) relative to the lower ones (850 °C) used for specimens HT2, the microstructural stability of samples HT1 is higher during long-term aging at temperatures greater than 827 °C.

4 Conclusions

1) The effect of the prior manufacturing route (casting or hot forming) is found to be insignificant on the overall coarsening behavior of the γ' particles.

2) The initial heat treatment has a major influence on the coarsening kinetics of the γ' particles.

3) In the temperature range of 790−827 °C, IN939 cast/wrought-HT2 alloys have more microstructural stability, while in the temperature range of 827−910 °C, the initial heat treatment marked as HT1 provides more stable microstructure for the cast or wrought IN939 superalloy.

4) The growth of γ' particles in the cast or wrought IN939 superalloy follows the LSW equation in the temperature range of 790−910 °C up to 1500 h. This shows that the volume diffusion of alloying elements controls particles growth rate.

5) An increase of 120 °C in aging temperature increases the growth rate factor by 21−27 times.

6) Primary MC carbides in the microstructure of cast or wrought IN939 superalloy transform to η phase and $M_{23}C_6$ carbides after prolonged aging at 790 °C. On the contrary, these primary carbides transform to γ' phase and $M_{23}C_6$ phases after long-term aging at 850−910 °C.

References

[1] ARDELL A J, NICHOLSON R B. The coarsening of γ' in Ni−Al alloys [J]. Journal of Physics and Chemistry of Solids, 1966, 27(11−12): 1793−1794.

[2] van der MOLEN E H, OBLAK J M, KRIEGE O H. Control of γ' particle size and volume fraction in the high temperature superalloy Udimet 700 [J]. Metallurgical Transactions, 1971, 2: 1627−1633.

[3] LIU L R, JIN T, LIU J L, SUN X F, HU Z Q. Effect of ruthenium on γ' precipitation behavior and evolution in single crystal superalloys [J]. Transactions of Nonferrous Metals Society of China, 2013, 23(1): 14−22.

[4] LI X, SAUNDERS N, MIODOWNIK A P. The coarsening kinetics of γ' particles in nickel-based alloys [J]. Metallurgical and Materials Transactions A, 2002, 33(11): 3367−3373.

[5] HUANG Y, WANG L, LIU Y, FU S M, WU J T, YAN P. Microstructure evolution of a new directionally solidified Ni-based superalloy after long-term aging at 950 °C up to 1000 h [J]. Transactions of Nonferrous Metals Society of China, 2011, 21(10): 2199−2204.

[6] COAKLEY J, BASOALTO H, DYE D. Coarsening of a multimodal nickel-base superalloy [J]. Acta Materialia, 2010, 58(11): 4019−4028.

[7] DAVIES C K L, NASH P G, STEVENS R N, YAP L C. Precipitation in Ni−Co−Al alloys [J]. Journal of Materials Science, 1985, 20(8): 2945−2957.

[8] ROBSON J D. Modeling competitive continuous and discontinuous precipitation [J]. Acta Materialia, 2013, 61(20): 7781−7790.

[9] GES A M, FORNARO O, PALACIO H A. Coarsening behaviour of a Ni-base superalloy under different heat treatment conditions [J]. Materials Science and Engineering A, 2007, 458(1−2): 96−100.

[10] KIM H T, CHUN S S, YAO X X, FANG Y, CHOI J. Gamma prime (γ') precipitating and ageing behaviours in two newly developed nickel-base superalloys [J]. Journal of Materials Science, 1997, 32(18): 4917−4923.

[11] BALIKCI E, ERDENIZ D. Multimodal precipitation in the

superalloy IN738LC [J]. Metallurgical and Materials Transactions A, 2010, 41(6): 1391−1398.
[12] LI H, ZUO L, SONG X, WANG Y, CHEN G. Coarsening behavior of γ′ particles in a nickel-base superalloy [J]. Rare Metals, 2009, 28(2): 197−201.
[13] WAHL J B, HARRIS K. Advanced Ni base superalloys for small gas turbines [J]. Canadian Metallurgical Quarterly, 2011, 50(3): 207−214.
[14] SJOBERG G, IMAMOVIC D, GABEL J, CABALLERO O, BROOKS J W, FERTE J, LUGAN A. Evaluation of the IN 939 alloy for large aircraft engine structures [C]//Superalloys 2004. Warrendale, PA: TMS, 2004: 441−450.
[15] JAHANGIRI M R, ARABI H, BOUTORABI S M A. Development of wrought precipitation strengthened IN939 superalloy [J]. Materials Science and Technology, 2012, 28(12): 1470−1478.
[16] JAHANGIRI M R, ARABI H, BOUTORABI S M A. High-temperature compression behavior of cast and homogenized IN939 superalloy [J]. Metallurgical and Materials Transactions A, 2013, 44(4): 1827−1841.
[17] JAHANGIRI M R, BOUTORABI S M A, ARABI H. Study on incipient melting in cast Ni base IN939 superalloy during solution annealing and its effect on hot workability [J]. Materials Science and Technology, 2012, 28(12): 1402−1413.
[18] JAHANGIRI M R, ARABI H, BOUTORABI S M A. Investigation on the dissolution of η phase in a cast Ni-based superalloy [J]. International Journal of Minerals, Metallurgy, and Materials, 2013, 20(1): 42−48.
[19] LIU Y, HU R, LI J, KOU H, LI H, CHANG H, FU H. Deformation characteristics of as-received Haynes230 nickel base superalloy [J]. Materials Science and Engineering A, 2008, 497: 283−289.
[20] LIN Y C, CHEN X M. A critical review of experimental results and constitutive descriptions for metals and alloys in hot working [J]. Materials and Design, 2011, 32(4): 1733−1759.
[21] KANG F W, ZHANG G Q, LI Z, SUN J F. Hot deformation of spray formed nickel base superalloy using processing maps [J]. Transactions of Nonferrous Metals Society of China, 2008, 18(3): 531−535.
[22] LVOV G, LEVIT V I, KAUFMAN M J. Mechanism of primary MC carbide decomposition in Ni-base superalloys [J]. Metallurgical and Materials Transactions A, 2004, 35(6): 1669−1679.
[23] ZHAO S, XIE X, SMITH G D, PATEL S J. Microstructural stability and mechanical properties of a new nickel-based superalloy [J]. Materials Science and Engineering A, 2003, 355(1−2): 96−105.
[24] SIMS C T, STOLOFF N S, HAGEL W C. Superalloys II [M]. New York: John Wiley and Sons, 1987.
[25] DONACHIE M J, DONACHIE S J. Superalloys: A technical guide [M]. Materials Park, OH: ASM International, 2002.
[26] CAMPBELL C E, BOETTINGER W J, KATTNER U R. Development of a diffusion mobility database for Ni-based superalloys [J]. Acta Materialia, 2002, 50(4): 775−792.
[27] BALDAN A. Review: Progress in Ostwald ripening theories and their applications to nickel-base superalloys. Part I: Ostwald ripening theories [J]. Journal of Materials Science, 2002, 37(11): 2171−2202.
[28] JENA A K, CHATURVEDI M C. The role of alloying elements in the design of nickel-base superalloys [J]. Journal of Materials Science, 1984, 19(10): 3121−3139.
[29] LIU J L, JIN T, YU J J, SUN X F, GUAN H R, HU Z Q. Effect of thermal exposure on stress rupture properties of a Re bearing Ni base single crystal superalloy [J]. Materials Science and Engineering A, 2010, 527(4−5): 890−897.
[30] TILEY J, VISWANATHAN G B, SRINIVASAN R, BANERJEE R, DIMIDUK D M, FRASER H L. Coarsening kinetics of γ′ precipitates in the commercial nickel base superalloy René 88 DT [J]. Acta Materialia, 2009, 57(8): 2538−2549.
[31] DELARGY K M, SMITH G D W. Phase composition and phase stability of a high-chromium nickel-based superalloy IN939 [J]. Metallurgical Transactions A, 1983, 14(9): 1771−1783.

两种不同方法制备的 IN939 高温合金在长时间时效过程中的组织稳定性的比较

M. R. JAHANGIRI[1], H. ARABI [2], S. M. A. BOUTORABI [2]

1. Metallurgy Department, Niroo Research Institute, Tehran 14686, Iran;
2. School of Metallurgy and Materials Engineering, Iran University of Science and Technology, IUST, Tehran 16846-13114, Iran

摘　要：采用光学显微镜、扫描电子显微镜及能谱分析对两种不同方法制备的 IN939 高温合金在高温、长时间时效过程中的组织稳定性进行研究。结果表明，γ′粒子的粗化行为主要受到初始热处理条件的影响，而之前的制备方法(铸造或热变形)的影响不明显，若有，也只是对 γ′粒子的粗化动力学有影响。在 790~827 °C 的温度范围内，铸态或锻态 IN939 合金样品都有比较好的组织稳定性。在 827~910 °C 的温度范围内，采用初始热处理条件 HT1 的样品不管是在铸态还是在锻态都有比较好的组织稳定性。

关键词：镍基高温合金；IN939 高温合金；长时间粗化；制备方法；热处理；γ′粒子；碳化物

(Edited by Hua YANG)